Review Article

Radiologic and pathologic correlation of anterior mediastinal lesions

Lea Azour[1], Andre L. Moreira[2], Sophie L. Washer[1], Jane P. Ko[1]

[1]Department of Radiology, [2]Department of Pathology, NYU Langone Health, New York, NY, USA

Contributions: (I) Conception and design: L Azour, JP Ko, AL Moreira; (II) Administrative support: None; (III) Provision of study materials or patients: All authors; (IV) Collection and assembly of data: L Azour, AL Moreira, SL Washer; (V) Data analysis and interpretation: All authors; (VI) Manuscript writing: All authors; (VII) Final approval of manuscript: All authors.

Correspondence to: Lea Azour. Department of Radiology, NYU Langone Health, 660 First Avenue, New York, NY 10016, USA.
Email: Lea.Azour@nyulangone.org.

Abstract: Anterior mediastinal lesions while rare, are heterogeneous in etiology, with broad differential considerations that may be narrowed by drawing on discriminating clinical, radiologic, and histopathologic features. This manuscript will review the radiographic and pathologic correlation of anterior mediastinal lesions of thymic, lymphomatous, and germ-cell origin.

Keywords: Anterior mediastinum; prevascular; thymus; germ-cell; radiology; pathology

Received: 12 September 2019; Accepted: 30 September 2019; Published: 25 March 2020.
doi: 10.21037/med.2019.09.05
View this article at: http://dx.doi.org/10.21037/med.2019.09.05

Introduction

Anterior mediastinal masses are rare and account for approximately 50% of all mediastinal lesions (1), with an estimated prevalence of nearly one percent in the general population (2). Management of patients with anterior mediastinal masses incorporates clinical, laboratory and imaging features (*Table 1*) to first derive the most likely differential diagnoses and disease extent, and secondly, direct histopathologic investigation in terms of site and type of sampling, such as core biopsy or flow cytometry. Beyond definitive diagnosis, histopathology is necessary for disease staging and confers prognostic information.

Anterior mediastinal lesions are heterogeneous etiologically, which adds to the complexity of the site. An understanding of the clinical context, laboratory results, and discriminating imaging and pathological features is needed for multidisciplinary diagnosis. This manuscript will provide a thorough radiology-pathology correlative review of common anterior mediastinal masses, including pearls and pitfalls encountered in multimodality imaging and histopathology diagnosis.

Mediastinal compartmental anatomy

The mediastinum is conventionally categorized into three compartments, anterior, middle and posterior. The majority of early mediastinal classification schemes were based on non-anatomic boundaries drawn from the lateral chest radiograph (16). In 2017, the International Thymic Malignancy Interest Group (ITMIG) developed a standard classification based on cross-sectional, multi-detector CT (MDCT) imaging landmarks (16), introducing prevascular (anterior), visceral (middle) and paravertebral (posterior) compartments.

According to ITMIG, the prevascular space, or anterior mediastinum, begins at the posterior cortex of the sternum and is bordered laterally by the medial parietal pleura on both sides. The prevascular space does not include the internal mammary vessels. The posterior margin is the anterior aspect of the pericardium as it wraps around the heart. Typical anterior mediastinal contents include thymus, mediastinal fat, lymph nodes, and the left brachiocephalic vein.

The middle mediastinal, or visceral, compartment

Table 1 Prevascular mediastinal lesions

Lesion type	Clinical and laboratory findings	Imaging findings	Histopathology features
Thymic epithelial neoplasms			
Thymoma	(I) 40–60 years. (II) Equal gender predilection (3). (III) Association with autoimmune and paraneoplastic syndromes. (IV) Myasthenia gravis (MG) in 30–50%; 10–15% with MG have thymoma (4)	(I) CT: often unilateral smooth, encapsulated soft tissue density lesion, however may be cystic; calcification, necrosis, and irregular margins more common in non-encapsulated, invasive thymomas. (II) MRI: useful to discern or exclude soft tissue in cystic thymomas or high attenuation thymic cysts, respectively. (III) Nuclear medicine: may lack or demonstrate FDG-avidity on PET/CT	Dual population of cells: thymic epithelial cells (keratin positive by immunohistochemistry, IHC) and immature thymic lymphocytes (TdT positive by IHC)
Thymic carcinoma	(I) 6th decade. (II) Slight male predilection. (III) Up to 50% have distant metastases at diagnosis (3)	(I) CT: more likely to demonstrate invasive features, lymphadenopathy, pleural/pericardial effusions, and distant metastases. (II) MRI: both T1 and T2 hyperintense relative to muscle, however calcification, hemorrhage, cystic change or necrosis may cause signal heterogeneity	Histological features are similar to carcinomas of other organs. Most thymic carcinoma cells are positive for CD5 and CD117 by IHC
Thymic neuroendocrine tumor	(I) 3:1 male to female predilection (5). (II) Half functionally active, most often associated with endocrinopathies such as Cushing syndrome due to ectopic ACTH; association with multiple neuroendocrine neoplasia (MEN) type 1 (5,6). (III) 50–75% may have regional or distant metastases (3)	(I) CT: commonly large and infiltrative (7); calcification in up to 30% (3); avid enhancement of non-necrotic areas. (II) MRI: similar T1 and T2 signal characteristics in comparison to thymoma, iso- to hyperintense on T1 and hyperintense on T2 (7). (III) Nuclear medicine: uptake on somatostatin-receptor imaging such as Indium-111 Octreoscan and Gallium-68 Dotatate PET/CT, however not specific as thymoma and thymic carcinoma may also demonstrate uptake	Plasmacytoid cells with “salt and pepper” chromatin pattern. Cytoplasm can be granular. Positive for neuroendocrine markers (chromogranin, synaptophysin and CD56)
Lymphoproliferative			
Hodgkin lymphoma	(I) Most common 2nd–4th decades. (II) Female predilection. (III) Arises from thymus and/or lymph nodes	(I) CT: large mass in thymic region often involving contiguous prevascular, paratracheal and subaortic, often also lower cervical and supraclavicular lymph nodes (3); may directly invade pulmonary parenchyma. (II) MRI: adenopathy is T2 hyperintense. (III) Nuclear medicine: FDG-PET used for staging and monitoring. (IV) Calcification rare in untreated lymphoma	(I) Nodular sclerosis type is the most common in the mediastinum. (II) Reed-Sternberg cells are the hallmark for the diagnosis
Primary mediastinal (thymic) large B-cell lymphoma	(I) Young adults in 3rd–4th decades. (II) Female predilection (3)	CT: large mass that may infiltrate pericardium, pleura, pulmonary parenchyma, chest wall	(I) Presence of irregular fibrosis is the hallmark of the diagnosis. (II) The tumor is confined to the mediastinum. (III) Similar IHC profile to large B cell lymphoma originating from other locations
T-lymphoblastic lymphoma (T-LBL)	(I) Adolescents and young adults. (II) Male predilection (3)	CT: large rapidly growing mass involving thymus, extracapsular mediastinal soft tissue, mediastinal lymph nodes	(I) Small to medium size lymphocytes with round nuclei and small nucleoli; numerous mitotic figures are present. (II) Tumor cells are positive for TdT by IHC

Table 1 (*continued*)

Table 1 (*continued*)

Lesion type	Clinical and laboratory findings	Imaging findings	Histopathology features
Germ cell tumors (GCT)			
Teratoma	(I) Equal gender predilection (3). (II) Often asymptomatic; may have symptoms in relation to lesion size; trichoptysis or expectoration of other tumoral contents via fistula with bronchi can occur rarely. (III) Association with Klinefelter syndrome. (IV) No elevation in beta-HCG or alpha-fetoprotein (AFP)	(I) CT: mass containing components of varying attenuation including fluid, soft tissue, calcium and/or fat; fat-fluid level highly specific (8), bone or tooth diagnostic. (II) MRI: T1 fat saturation sequence to identify macroscopic fat; calcification may cause susceptibility artifact	(I) Tumor composed of epithelial, mesenchymal and neural tissue; not all components need to be present for the diagnosis. (II) There is no specific IHC for the diagnosis
Seminomatous GCT	(I) Almost exclusively in men. (II) 3rd–4th decade. (III) Elevated beta-HCG in approximately one third of patients; LDH may be elevated (3)	(I) CT: often homogeneous circumscribed mass with mild enhancement (9). (II) Pulmonary metastases common	(I) Large cells with prominent nuclei, often associated with lymphocytes. (II) Granulomatous reaction can be present. (III) Tumor cells are positive for SALL4, OCT4, D2-40 and CD117
Non seminomatous GCT	(I) Primarily children, young men. (II) Elevated AFP in 80%, beta-hCG in 30%; LDH may be elevated (3). (III) Association with Klinefelter syndrome, hematologic malignancies	(I) CT: heterogeneous, irregularly marginated mass with areas of hemorrhage, necrosis, invasion (9). (II) Pulmonary metastases common	(I) Yolk sac tumor, choriocarcinoma, and embryonal carcinoma are high grade malignant epithelial neoplasms. (II) The diagnosis is confirmed by specific IHC stains and correlation with serum markers
Miscellaneous anterior mediastinal lesions			
Thymic hyperplasia	(I) True (rebound) thymic hyperplasia as sequela of physiologic stressors such as illness, injury, chemo/ radiotherapy (10). (II) Thymic lymphoid hyperplasia most often in setting of systemic immunologic conditions including hyperthyroidism, autoimmune disease such as myasthenia gravis, collagen vascular disease, HIV (11)	(I) CT: may be homogeneously enlarged thymic soft tissue or heterogeneous due to interspersed fat. (II) MRI: chemical shift imaging demonstrates loss of signal on opposed phase T1-weighted sequence due to presence of microscopic fat, characteristic of thymic hyperplasia. (III) Nuclear medicine: No uptake on somatostatin receptor imaging as seen in thymic epithelial neoplasms; may demonstrate physiologic, low level FDG-avidity	(I) Histologic section shows normal thymic structures, lobules are interspersed with adipose tissue. (II) Well-developed lymphoid follicles are seen in follicular hyperplasia
Thymolipoma	(I) Often large mass in young demographic. (II) Uncommonly in association with myasthenia gravis (12); case reports of thymoma arising within thymolipoma (13-15)	CT: adipose with intermixed thymic soft tissue; encapsulated and often conforming to anterior mediastinal structures; may have tumor pedicle and most often located at inferior aspect prevascular compartment (12)	Circumscribed tumor composed of mature fat admixed with islands of normal thymic tissue
Thyroid	Anterior mediastinal thyroid tissue may be due to substernal extension of goiter, or less commonly ectopic thyroid tissue discontinuous from cervical thyroid	(I) CT: often the same attenuation as cervical thyroid tissue. (II) Nuclear Medicine: Tc-99m pertechnetate, I-123 or I-131 scans may characterize tissue as thyroid	(I) Irregular sized thyroid follicles containing colloid. (II) Cells are positive for TTF-1 and PAX-8 by IHC
Ectopic parathyroid	Elevated PTH/hypercalcemia can occur	(I) CT and MRI: often hypervascular. (II) Nuclear Medicine: Tc-99m Sestamibi parathyroid scintigraphy	(I) Sheets of bland cells with clear and/ or oncocytic cytoplasm admixed with fat; delicate fibrous bands can be seen. (II) Cells are positive for parathyroid hormone by IHC

includes the remainder of vascular structures: superior vena cava, ascending and descending thoracic aorta, and intrapericardial pulmonary arteries. In addition, the visceral compartment contains the pericardium, heart, trachea, esophagus, thoracic duct, and lymph nodes. It extends posteriorly to a plane 1 cm beyond the anterior aspect of the vertebral bodies. The posterior, or paravertebral, compartment includes the thoracic spine and paravertebral soft tissues extending to the lateral point of the transverse processes.

Anterior mediastinal masses may be categorized as neoplastic or nonneoplastic, according to anatomic structure of origin (3), or by tissue attenuation on CT or signal characteristics on MRI (17). This manuscript will review anterior mediastinal differential considerations based on tissue of origin.

Thymic lesions

Thymic lesions comprise the majority of clinically-encountered anterior mediastinal masses, with incidence estimated at 40% of all mediastinal lesions (11), including both noninvasive and invasive histopathologies.

Thymic epithelial neoplasms

The classification of thymic tumors was most recently updated in the 4th edition of the World Health Organization (WHO) Classification of Tumours of the Lung, Pleura, Thymus and Heart (3). Thymic epithelial neoplasms include thymoma, thymic carcinoma, and thymic neuroendocrine tumors. Thymic epithelial neoplasms follow a tumor-node-metastasis (TNM) staging system (4), which correlates with disease recurrence and survival (18).

Thymoma

Thymoma is the most common primary mediastinal tumor in adults, with incidence seven to eight times that of thymic carcinoma (3). Thymomas most commonly occur in individuals 40–60 years of age, with a roughly equal gender distribution (3). Incidence is higher in Asians and Pacific Islanders based on Survival, Epidemiology and End Results (SEER) data from the United States (3), with overall incidence 0.13 per 100,000 (19).

Many autoimmune and paraneoplastic disorders are associated with thymoma. Myasthenia gravis is the most common, occurring in 30–50% of patients with thymoma; conversely, 10–15% of individuals with myasthenia gravis have underlying thymoma (4). Other paraneoplastic and autoimmune syndromes include neuromuscular, hematologic, connective tissue, dermatologic, and endocrine disorders (3,20,21). Thymoma has also been associated with increased risk of B-cell non-Hodgkin lymphoma, and sarcoma (19).

Thymoma is a malignant neoplasm with many different histological features. Treatment and prognosis depend on staging, which is based on the degree of local invasion and tumor spread, and not on histological classification. Histologically, thymomas are classified based on the morphological characteristics of the neoplastic cells. Type A thymomas are composed of spindled cells, whereas Type B thymomas have polygonal cells. Type B thymomas are sub-classified depending on the amount of infiltrating thymic lymphocytes, with lymphocyte-rich Type B1 and lymphocyte-poor Type B3. Type B2 has intermediate proportions of lymphocytes. A detailed classification scheme and diagnostic features are provided in the WHO classification (3).

CT plays a major role in the diagnosis and characterization of thymoma. CT imaging has been found to have 88.5% sensitivity and 77% specificity for thymoma, based on a case series of 104 patients with myasthenia gravis (22). On imaging, thymoma may not conform to the shape of normal thymic tissue. Thymoma usually presents as a smoothly-circumscribed, encapsulated soft-tissue density lesion (3) (*Figure 1*), often homogeneous in enhancement. Calcification may be seen, and is more common in invasive rather than noninvasive (encapsulated) thymomas (23). Areas of necrosis, cystic change, or hemorrhage are less common (3).

Cystic thymomas (*Figure 2*) and benign thymic cysts may mimic one another, with MRI very useful for differentiating these entities. MRI may identify fibrous internal septae, soft tissue mural nodularity, and enhancement, as well as characterize fluid as simple, proteinaceous, or hemorrhagic. Any foci of hemorrhage would appear T1 hyperintense. Soft tissue components are hypo to iso-intense on T1-weighted images, and hyperintense on T2-weighted sequencing. In addition to MRI's superiority to CT in discerning soft tissue components and fluid characterization, it may also be helpful in distinguishing local invasion. PET/CT does not have a large role in terms of diagnostic specificity.

Certain morphologic and imaging features can indicate advanced disease (*Figure 3*). Key findings to identify include mediastinal pleural invasion or pericardial extension and invasion, loss of fat planes between mediastinal vasculature

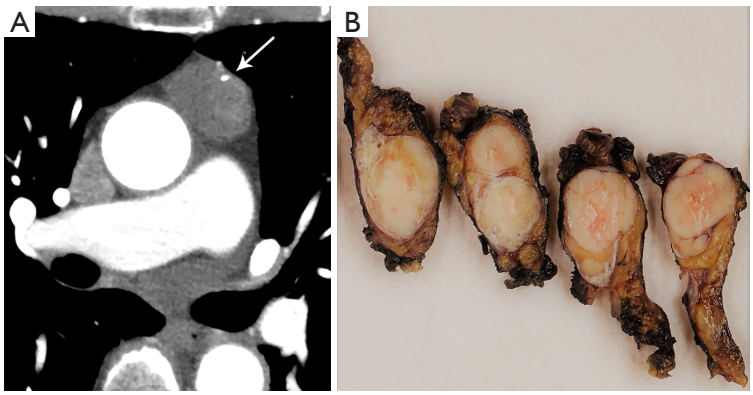

Figure 1 Encapsulated thymoma. A 75-year-old woman with anterior mediastinal mass incidentally noted on coronary computed tomographic angiography (CCTA). (A) Contrast enhanced CCTA shows a well-circumscribed lesion in the prevascular compartment, with small internal calcification (arrow) and mild enhancement most conspicuous at its left lateral aspect; (B) thymectomy specimen of the tumor demonstrates a lobulated tumor within the thymus. Note the tumor is circumscribed and does not appear to invade into the adipose tissue.

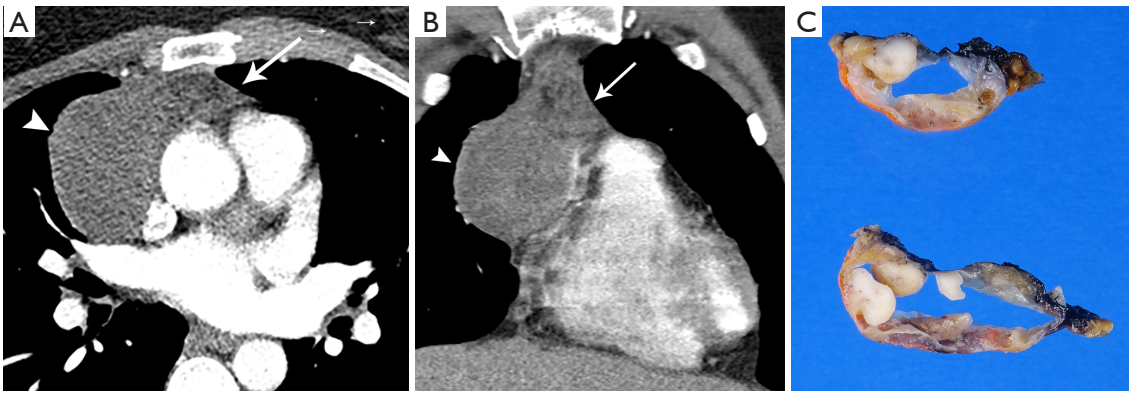

Figure 2 Cystic thymoma. A 34-year-old woman presenting with pleuritic chest pain and new anterior mediastinal mass since imaging two years prior. (A and B) Contrast-enhanced chest CT pulmonary angiogram (CTPA) axial (A) and coronal (B) images demonstrate thymic soft tissue in the anterior mediastinum (arrow), with a right anterior mediastinal mass of intermediate density (30 HU) in the right thymus. Mass is circumscribed, with a round cystic component (arrowhead) impressing on adjacent vessels and heart. (C) Thymectomy specimen, cut surface, shows a unilocular cyst with soft tissue nodularity in the cyst wall. Histological examination of the nodules confirms a B2 thymoma.

and viscera, and nodal or metastatic lesions. Pleural, pericardial or distant metastases are exceedingly rare in types A and AB thymoma. Local recurrence/spread is estimated to occur in less than 5% of type B1, 11% of type B2, and 18% of type B3 thymomas; distant metastases occur in approximately 3% with types B2 and B3 thymomas (3).

Biopsy of thymomas is often reserved for advanced stage (invasive thymoma), as histological diagnosis is required for systemic therapy. Smaller tumors confined to the mediastinum are often resected without a preceding biopsy, unless an alternative diagnosis is suspected. Mediastinal biopsies are safe and efficient (24), especially with new minimally-invasive techniques including core and aspiration biopsies.

The hallmark of the histological diagnosis of thymoma is the presence of two cell populations, one comprised of epithelial cells and another of immature lymphocytes (*Figure 4*). However, this classic feature may not be present in many cases due to sampling and histological variation. Immunohistochemical (IHC) stains are very helpful as the thymocyte epithelial cells are positive for keratin, whereas immature lymphocytes are positive for TdT. There must be close co-localization of the two cell populations, as the markers individually are not specific for the diagnosis

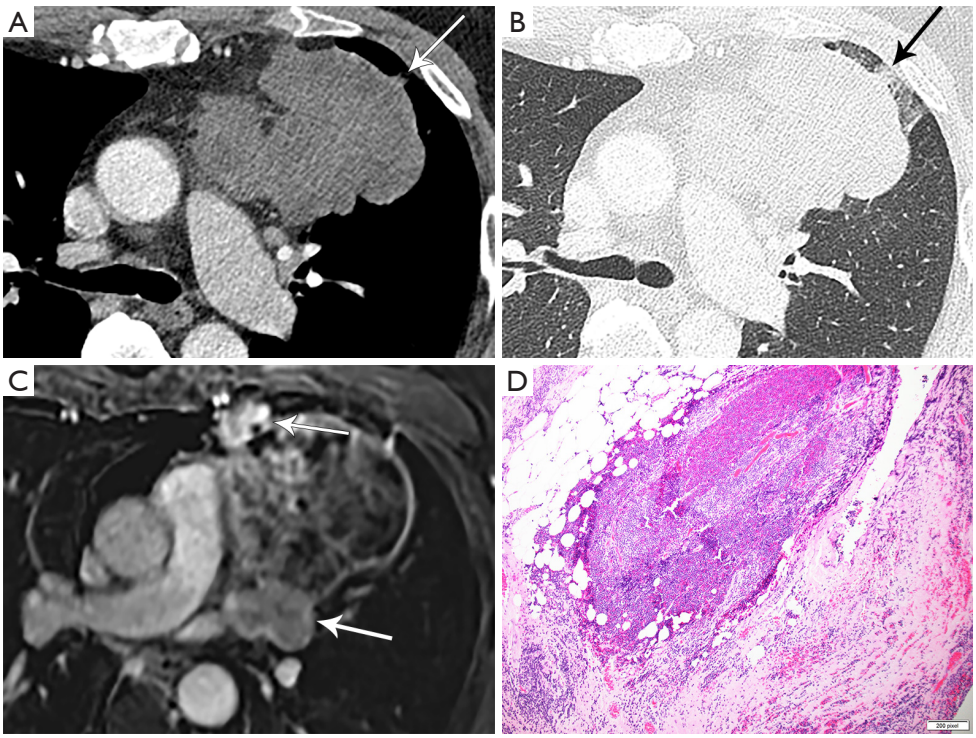

Figure 3 Invasive thymoma. A 67-year-old man with incidentally found mass on routine radiograph, status post 3 months of chemotherapy for invasive thymoma. Imaging performed prior to planned resection. (A) Contrast enhanced axial CT image demonstrate a predominately smoothly-marginated heterogeneously enhancing left anterior mediastinal mass with small foci of capsular irregularity and extracapsular soft tissue extension into the lung parenchyma (arrow), correlating with invasion on pathology. Imaging also revealed foci of calcification and low density cystic components (not shown). (B) Lung windows show extracapsular soft tissue and ground glass opacity in the left upper lobe parenchyma adjacent the mass (arrow). (C) Axial post-contrast subtraction MR image demonstrates heterogeneous and confluent nodular areas of enhancement (arrows) compatible with viable tumor, with hypointense non-enhancing foci of cystic degeneration and necrosis compatible with chemotherapy treatment effect. (D) Invasive thymoma, image shows a B2 thymoma that had invaded the fibrous capsule and lies within peri-thymic adipose tissue (H&E stain).

of thymoma and can be seen in other entities. As an example, TdT positive lymphocytes are present in acute lymphoblastic lymphoma, a common lymphoproliferative disorder of the mediastinum in children and younger adults. The immature (TdT positive) lymphocytes are also seen in metastatic thymoma, a useful diagnostic feature for the diagnosis of thymoma outside of the mediastinum.

Thymic carcinoma

Thymic carcinoma accounts for 17–22% of thymic epithelial neoplasms, with the vast majority (70–79%) classified as squamous cell carcinoma (3). Additional less common histopathologic subtypes include basaloid, mucoepidermoid, clear cell, sarcomatoid, and NUT carcinomas, among others. Thymic carcinoma most commonly affects individuals in their 50s, with a slight male predominance (3). Thymic carcinoma has a poorer prognosis than thymoma and often presents at a more advanced disease stage. Paraneoplastic syndromes are less common than with thymoma (25).

On imaging, thymic carcinoma is more likely to be poorly or irregularly marginated and more likely to have internal heterogeneity due to calcification or cystic/necrotic change (*Figure 5A*). Thymic carcinomas are often associated with pericardial or pulmonary parenchymal invasion (40%), pleural invasion (30%), and vascular invasion (20%) into the superior vena cava or brachiocephalic veins (3). Additionally, a higher proportion, approximately 19–50%, present with distant metastases, most often to bone, liver, lung, and adrenal gland, at time of diagnosis in comparison to thymoma (3). Pericardial effusion, pleural effusion, or enlarged lymph nodes are also more likely with thymic

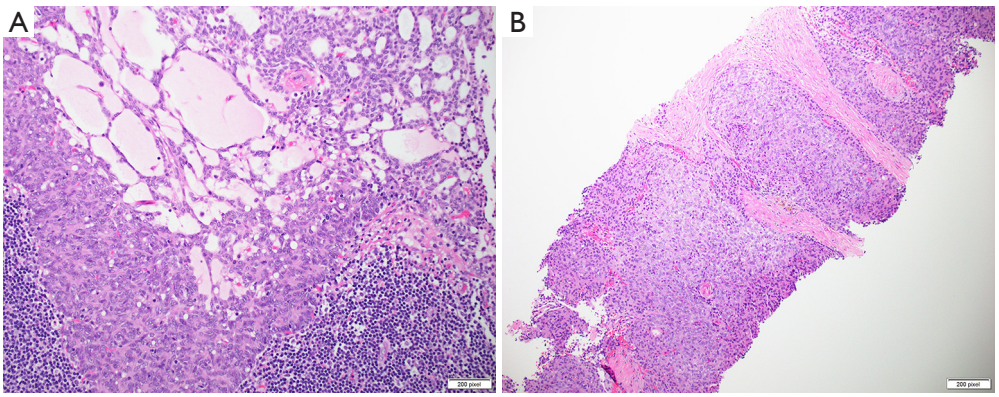

Figure 4 Thymoma AB. (A) Histology image shows a thymoma type AB. The clusters of epithelial cells are spindled shaped (pale cells), and there are multiple microcystic structures within the tumor. Type A thymomas have several histological patterns, but the presence of spindled shaped cells is characteristic. This tumor is classified as Type AB because, in addition to the areas of spindled cells, there are areas rich in lymphocytes (blue cells) that are clustered within the thymoma (type B1). An Immunohistochemical stain for keratin would highlight the epithelial cells with the B1 component. (B) Core biopsy of a B3 thymoma. These tumors are epithelial-rich with sparse thymic lymphocytes (TdT positive lymphocytes). Contrary to type A thymomas, the epithelial cells in B3 thymomas are polygonal shaped. Most thymomas have a lobulated growth pattern with thick bands of fibrosis, as seen here. Thymomas types A and B3 appear pink on H&E stains, whereas B1 and B2 thymomas that are rich in lymphocytes appear blue. H&E stain.

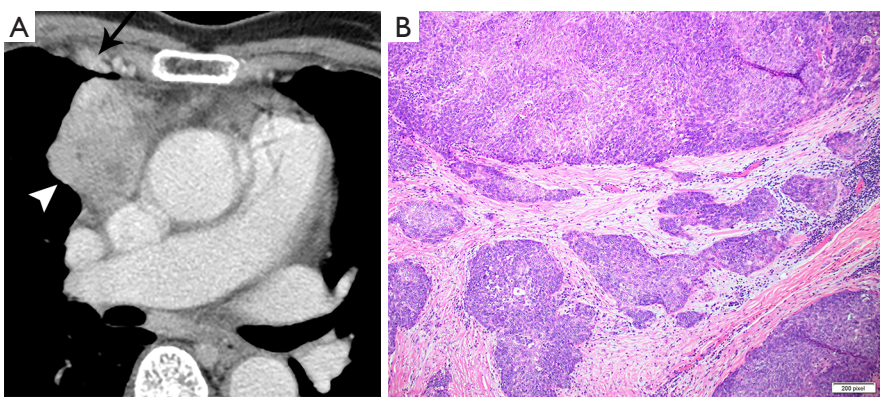

Figure 5 Thymic carcinoma. A 72-year-old woman with chest pain and dyspnea. (A) Contrast-enhanced axial CT image demonstrates a heterogeneously enhancing hypervascular right anterior mediastinal mass (arrowhead), demonstrating greater enhancement than a typical thymoma. In addition, there is an enhancing metastatic right internal mammary lymph node (arrowhead). (B) Histology from the excised mass shows a tumor with infiltrative growth patterns, smaller irregular clusters of tumor cells in a dense, desmoplastic stroma. The tumor cells exhibit significant atypia (H&E stain). These findings are diagnostic of squamous cell carcinoma. Immunohistochemical stains show the tumor cells to be positive for CD5 and CD117, which confirm thymic origin.

carcinoma than thymoma.

Thymoma and thymic carcinoma have different MR characteristics. Thymic carcinomas are hyperintense on both T1 and T2 weighted images, distinct from the T1 hypointensity of thymomas, and there may be signal heterogeneity due to calcification, necrosis and/or hemorrhage. Soft tissue components will enhance on post-contrast images, and invasion into adjacent structures may be more clearly delineated. MR can identify distant metastatic disease in the pleura, lymph node stations, and bones included in the area imaged.

The histological diagnosis of thymic carcinoma is characterized by the clearly malignant features of the epithelial cells and the absence of TdT positive lymphocytes

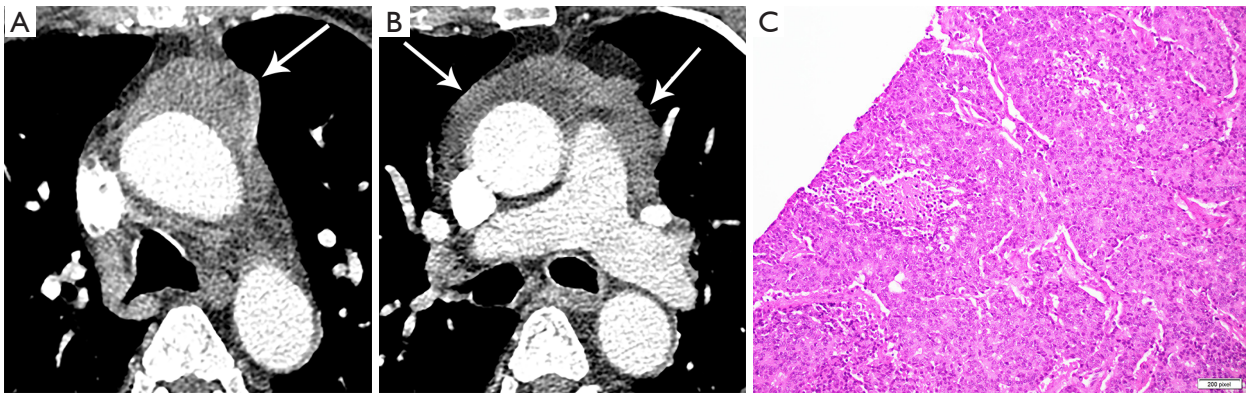

Figure 6 Thymic neuroendocrine tumor. A 65-year-old man with bone metastases and splenic lesion on MRI abdomen, presenting for CT chest to determine site of primary malignancy. (A) Contrast-enhanced axial CT image demonstrates a lobular heterogeneously enhancing anterior mediastinal mass (arrow). (B) Imaging at the level of the pulmonary artery bifurcation shows nodular pericardial thickening (arrows) and small pericardial fluid adjacent to and contiguous with mass, indicating pericardial involvement. Metastatic supraclavicular and mediastinal lymphadenopathy, and pulmonary metastases were also noted. (C) Core biopsy of the mediastinal tumor shows a tumor composed of cells with "salt and pepper chromatin" pattern (H&E stain). The cells form rosettes. A small focus of necrosis is seen. The differential diagnosis between typical and atypical carcinoid is problematic in a small biopsy, however the presence of the necrotic focus helps classify this tumor as an atypical carcinoid tumor. Atypical carcinoid tumors are the most common neuroendocrine tumors of the anterior mediastinum. The classification between typical and atypical carcinoid depends on mitotic counts as per the WHO.

(*Figure 5B*), in contrast to thymoma.

Thymic carcinomas can be positive for CD5 and CD117 by IHC stains in approximately 60% of cases (26).

Thymic neuroendocrine tumor

Thymic neuroendocrine tumor is a rare (2–5% of thymic neoplasms) but potentially aggressive neoplasm, including low-grade typical and intermediate-grade atypical carcinoids, and high-grade large cell neuroendocrine and small cell carcinoma (3). The diagnostic histological criteria for thymic neuroendocrine tumors are the same as their pulmonary counterpart (3).

On imaging, these lesions may be large (2–20 cm), heterogeneous and/or infiltrative masses (7) (*Figure 6*). The majority do not have a capsule on histopathology, and may be either circumscribed or invasive. Calcification is seen in 30% of typical carcinoids (3). Regions of necrosis or hemorrhage can occur in aggressive tumors with high mitotic activity (4,5). Non-necrotic components are expected to enhance avidly on cross-sectional imaging. Half of individuals with typical or atypical carcinoid will have regional nodal or distant metastases, and 10% with atypical carcinoid may show contiguous pleural or pericardial invasion (3). In distinction, three quarters of the more invasive large cell neuroendocrine carcinomas demonstrate local invasion or distant metastases (3). On MRI, these lesions will be T1 iso to hyperintense and T2 hyperintense, and can exhibit heterogeneous signal characteristics (7).

Thymic hyperplasia

Visualization of thymic tissue in the anterior mediastinum is a normal finding in young individuals. The thymus is a lymphoid organ responsible for T cell lymphopoiesis and is greatest in relative size in infancy, appearing biconvex and masslike on CT, often quadrilateral (10). With age, the thymic tissue regresses, becoming more triangular and conforming to the prevascular space, with a typical bilobed, triangular inverted V-shape, though variations such as uni- or tri-lobe may be seen (10).

Thymic involution and fatty replacement accelerates after puberty, with thymic soft tissue most often regressing by age 40. The size and CT attenuation of normal thymus in young adults (20–30 years) has been found to significantly differ based on gender, with greater thymic attenuation (more solid and less fatty), and thicker, quadrilateral geometry in young women (27).

There are two types of thymic hyperplasia: true thymic hyperplasia, synonymous with thymic rebound; and thymic lymphoid (follicular) hyperplasia. True or rebound thymic

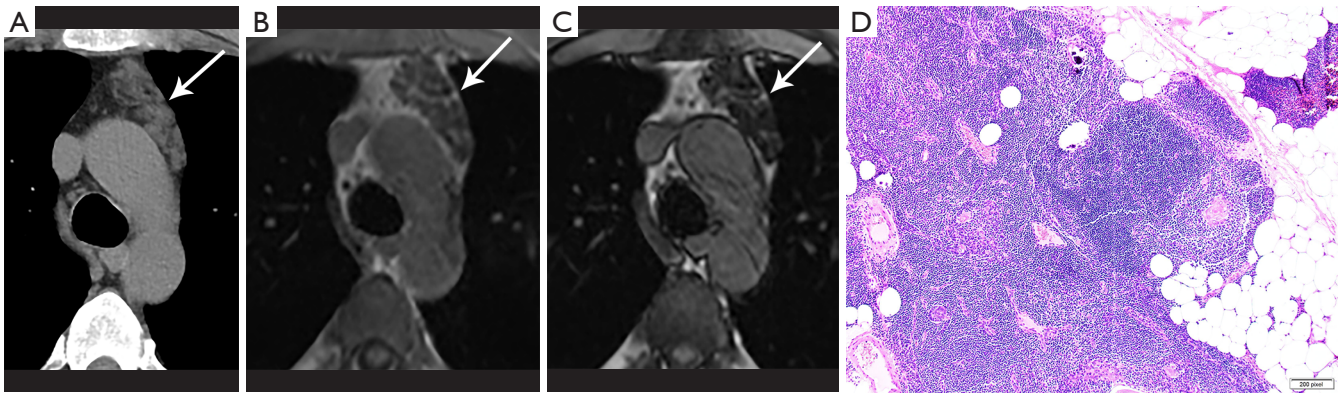

Figure 7 Thymic hyperplasia. A 55-year-old asymptomatic man. (A) Non-contrast chest CT demonstrates increased soft tissue confined to the anterior mediastinum (arrow). (B,C) Axial in-phase (B) and out-of-phase (C) images through the lesion demonstrate loss in signal on opposed phase sequence compatible with intravoxel fat, characteristic of thymic hyperplasia. Nonetheless, patient proceeded to resection. (D) Histological sections (H&E stain) show normal thymic structures that are disproportional in cellularity to the expected amount of thymic involution for a 55-year-old, consistent with true thymic hyperplasia. In follicular thymic hyperplasia, there are numerous lymphoid follicles that are composed of B-cells.

hyperplasia occurs most often as a sequela of stressors such as chemo- or radiotherapy, immunosuppression, illness or injury (10). Prevalence of rebound thymic hyperplasia after chemotherapy is not uncommon, reported in 11–37% (28-31). Thymic lymphoid hyperplasia most often occurs in the setting of systemic immunologic conditions including hyperthyroidism, autoimmune disease like myasthenia gravis (reportedly 65–77%), collagen vascular disease, or human immunodeficiency virus (HIV) (6).

On imaging, thymic hyperplasia should be suspected when there is new or increasing soft tissue in the thymic bed, or soft tissue greater than expected for age. The increased soft tissue may be heterogeneous in appearance due to interspersed fat (32), or homogeneous with often preservation of thymic morphology. Thymic hyperplasia can be triangular, bilobed, bipyramidal or quadrilateral morphologically (33), and in one series most often pyramidal in shape with convex margins (32). CT imaging features have not been shown to reliably distinguish between true and lymphoid hyperplasia, though a study of 29 individuals found CT attenuation to be significantly higher in those with lymphoid rather than true thymic hyperplasia, with an optimal threshold of 41.2 Hounsfield units (32).

Given thymic hyperplasia may be mass-like and mimic the appearance of thymic epithelial neoplasms, metastases, or lymphoma on CT, MR may be pursued for tissue characterization and may obviate the need for biopsy or resection. MR imaging with in- and out-of-phase sequences to evaluate for chemical shift, which is loss of signal intensity on opposed phase images, can identify the microscopic fat characteristic of thymic hyperplasia (*Figure* 7). Inaoka *et al*. reported uniform suppression of thymic tissue on opposed phase imaging with a chemical shift ratio (CSR) of <0.7 to identify thymic hyperplasia (34). Priola *et al*. also found CSR to be highly accurate in differentiating thymic hyperplasia from tumor (35). A pitfall to be aware of is that normal thymus in a young adult in which fatty involution has not yet begun may not demonstrate the expected CSR (36).

SUVmax has been shown to significantly differ between thymic hyperplasia, thymoma, and thymic carcinoma (37,38). Ambiguity on PET/CT may present however in differentiating thymic hyperplasia from recurrent malignancy in patients with history of chemotherapy (39). Adenopathy in multiple mediastinal locations and clinical context are useful to differentiate thymic hyperplasia from other etiologies in this scenario.

The histological diagnosis of thymic hyperplasia and thymoma is very difficult to render in a biopsy specimen due to overlapping characteristics (dual population of bland epithelial cells and immature lymphocytes). The differentiation of thymic hyperplasia from thymoma is best made on excisional biopsy. Thymic hyperplasia maintains the normal organotypic organization of the thymus, which is lost in thymoma. Resection of thymic hyperplasia is indicated in cases of Myasthenia gravis.

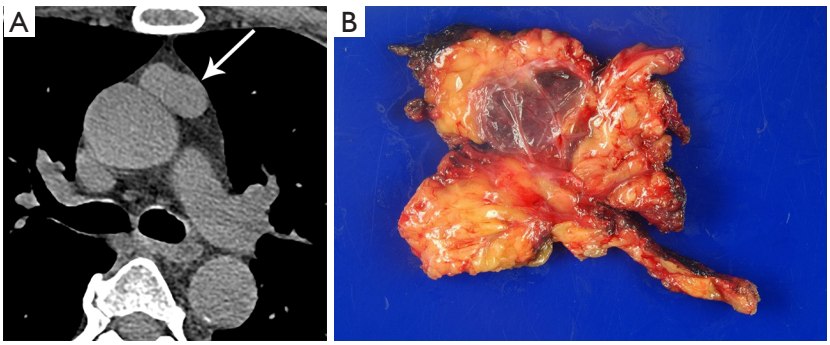

Figure 8 Thymic cyst. A 51-year-old man presenting for preoperative evaluation prior to coronary artery bypass grafting. (A) Axial non-contrast image demonstrates a well circumscribed 3 cm anterior mediastinal lesion, which while higher than simple fluid in attenuation (40 HU), nonetheless proved to be a thymic cyst rather than thymoma. When managing a smoothly marginated anterior mediastinal mass, preoperative MRI can be used to differentiate thymic soft tissue lesions from proteinacous thymic cysts. (B) Gross image of a unilocular thymic cyst reveals a translucent thymic cyst in the middle of the thymus. The cyst was lined by flat epithelium and contained involuting thymic tissue in its wall.

Thymic cyst

Thymic cysts are benign entities that rarely require resection, unless imaging is equivocal or lesion exerts mass effect on neighboring structures. Thymic cysts can be congenital or acquired, and uni- or multilocular.

Appearance on CT is often that of a fluid-attenuation cyst. On MRI, a simple cyst will display low T1 and high T2 signal intensity. However, cysts may be complex in terms of fluid attenuation or presence of septations. For this reason, diagnostic accuracy of CT for thymic cysts may be inferior to that of MRI (33,40) (*Figure 8*), particularly if a cyst is multiloculated or complex. MRI can characterize T1 hyperintense hemorrhagic or proteinaceous inflammation within a cyst, and exclude soft tissue or enhancing septations via post-contrast subtraction sequences.

Of note, thymic cysts may be associated with other prevascular lesions. For example, they may be seen in the setting of thymoma, with an incidence of 15% in a series of 54 resected thymomas (41), as well as thymic enlargement in the setting of lymphoma (42). Chemotherapy, radiotherapy or surgical intervention are other causes of acquired thymic cysts (10).

Lymphoma and lymphoproliferative processes

Hodgkin lymphoma (HL)

HL accounts for 30% of all lymphomas (43), with an overall bimodal distribution including median age 28 years and second peak at age 60–70 years (44). The nodular sclerosis subtype of classical HL comprises up to 70% of primary mediastinal lymphomas, most often presenting in patients in teenage years to mid-thirties (3). There is a female predilection, association with higher socioeconomic status, and similarly more commonly occurring in industrialized nations (3).

Mediastinal HL may involve lymph nodes, thymus or both. In a series of 43 patients, thymic enlargement was found in over half (56%) of individuals, with thymic and lymph node disease in 42%, and isolated thymic Hodgkin disease in 14% (42).

Mediastinal HL presents as large mass. Bulky disease is defined as a mass greater than or equal to 10 cm or spanning 1/3 of the transthoracic diameter (44). Mediastinal HL commonly involves contiguous prevascular, paratracheal and subaortic lymph nodes, and often also involves lower cervical and supraclavicular lymph nodes (3). It may directly invade pulmonary parenchyma or chest wall. On imaging, the presence of contiguous multistation enlarged thoracic lymphadenopathy may support lymphomatous etiology over a lesion of thymic epithelial origin. Calcification is rare in untreated lymphoma.

On MRI, while hypercellular lesions such as benign lymphadenopathy due to granulomatous processes are typically T2 hypo-intense, untreated lymphoma is a hypercellular exception and is T2 hyper-intense, with decline in signal intensity with treatment response, as the lesion becomes more collagenous/fibrotic (45).

There are four histopathologic subtypes of HL, including nodular sclerosis, mixed cellularity, lymphocyte rich, and

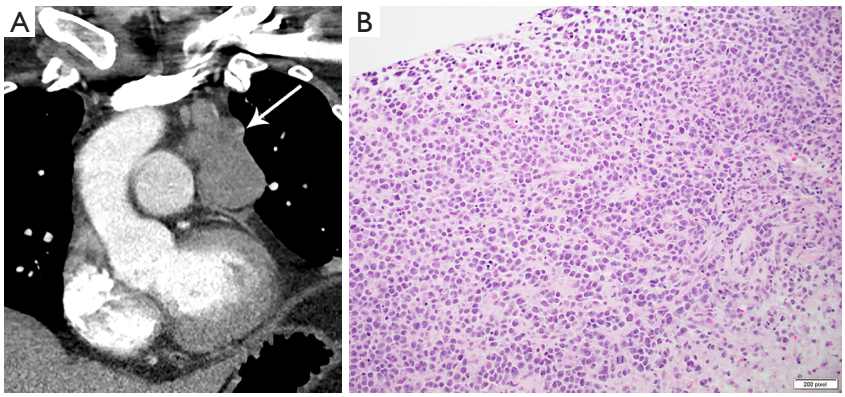

Figure 9 Primary Mediastinum Large B-Cell Lymphoma (PMLBCL). 49-year-old man with acute chest pain and dyspnea, presenting for CTPA. (A) Coronal contrast-enhanced CTPA image demonstrates a bulky soft tissue density mass in the thymic region (arrow). The presence of other mediastinal lymph nodes is helpful, and when the mass may represent a conglomeration. (B) Histological sections show a tumor composed by large cells with predominant nucleoli (H&E stain). The cell growth is in sheets. Focal fibrosis was seen (not shown). The tumor cells are positive for CD45 and CD20 by IHC. Other markers characteristic of large B-cell lymphoma are also positive. For the diagnosis of PMLBCL the tumor needs to be confined to the mediastinum. In distinction, if there is involvement of extra-mediastinal lymph nodes, the tumor should be classified as large B-cell lymphoma.

lymphocyte depleted. Identification of the Reed-Sternberg cell is requisite for the diagnosis. Nodular sclerosis (classical type) is the most common type in the mediastinum. The diagnosis may be challenging to render in a small biopsy specimen or cytology due to sampling, as the diagnostic Reed-Sternberg cells may not the present in the specimen. However, the presence of a fibrotic lesion with a mixed inflammatory background containing eosinophils should raise the suspicion for HL. If the diagnosis cannot be established, additional tissue should be procured. Reed-Sternberg cells can be characterized by IHC stains. The cells are positive for CD30 and CD15; CD20 and EBV positivity can also be seen in HL.

Non-Hodgkin lymphoma (NHL)

There are many subtypes of NHL that can affect the mediastinum. The mediastinum can be commonly involved by diffuse large B-cell lymphoma, follicular lymphoma, and marginal zone lymphomas (43). Of note, the incidence of NHL is 60–200 times greater in individuals with HIV depending on NHL subtype (43), and the prevalence of NHL is higher in developing countries. The most common primarily mediastinal NHLs include primary mediastinal large B-cell lymphoma (PMLBCL), and acute lymphoblastic lymphoma.

On imaging, NHL may be indolent with progressive lymphadenopathy and hepatosplenomegaly, or an aggressive rapidly growing mass. Lymphadenopathy is most often in the prevascular and paratracheal stations, though may involve additional nodal stations including subcarinal, hilar, posterior mediastinal, and retrocrural. NHL may demonstrate chest wall involvement through direct extension, or less commonly presenting as an isolated chest wall mass (46).

The suspicion for mediastinal lymphoma is highly influenced by demographic factors and clinical presentation. As in many lymphoproliferative disorders, the use of ancillary tests such as IHC and flow cytometry is essential, as morphological features alone are shared by many entities.

Primary mediastinal (thymic) large B-cell lymphoma (PMLBCL)

PMLBCL is a type of diffuse large B-cell NHL arising in the thymus, though also related to the nodular sclerosing type of HL given both originate from the thymic B cell (47,48). PMLBCL accounts for 10% of diffuse large B-cell lymphomas (DLBCL) (49), and accounts for 2–4% of NHL overall (43). PMLBCL occurs more frequently in young women (2:1 female to male ratio), and is often aggressive in terms of size and stage, with elevated lactate dehydrogenase levels (49); LDH is a prognostic factor in both HL and NHL.

On imaging, the mass of PMLBCL is located in the thymic region (*Figure 9*), often large and bulky, and may

invade the pericardium, pleura, or lungs, and involve supraclavicular and cervical lymph nodes (43). The aggressive nature of PMLBCL is reflected in its propensity to cause superior vena cava syndrome (43). Of note, involvement of other nodal regions or bone marrow involvement would preclude this diagnosis and rather indicate DLBCL with secondary mediastinal involvement (43). Pleural and pericardial effusions can occur, seen in approximately one third of patients (3).

The histological diagnosis is characterized by sheets or clusters of large malignant lymphocytes within dense fibrosis. Tumor cells are diffusely positive for CD20 and PAX-5 and have a high proliferation rate. The differential diagnosis also includes HL due to presence of fibrosis and the occasional Reed-Sternberg cells. However, PMBL lacks the classical inflammatory infiltrate seen in HL.

T-lymphoblastic lymphoma (T-LBL)

T-LBL is a rare aggressive neoplasm of T- cell precursors that affects predominantly adolescents and young adults, with a male predilection (3). Most cases are confined to the mediastinum (thymus and lymph nodes). When significant involvement of bone marrow and peripheral blood is present, the term acute lymphoblastic leukemia applies.

On imaging, the mass usually involves the thymus and mediastinal lymph nodes, with pleural or pericardial effusions. There is often extrathoracic lymphadenopathy and splenomegaly.

The histological diagnosis is characterized by the presence of small to medium-sized lymphocytes with round nuclei and small nucleoli. Mitotic figures and apoptotic bodies are frequent. IHC stains show the tumor cells to be positive for TdT and CD 99, which characterize immature T cells. In the vast majority of cases, rearrangement in T cell receptor genes is identified. The diagnosis can be challenging and is often a medical emergency due to rapid tumor growth and resultant compression of intrathoracic organs.

Lymphoma staging and response

The Cotswold revision of the Ann Arbor staging system classifies lymphoma based on nodal distribution of involvement (43), and is used for both HL and NHL. Stage I is involvement of one lymph node region or lymphoid organ; Stage II indicates two or more regions (mediastinum is a single region) on the ipsilateral side of diaphragm; Stage III disease involves lymph node regions on both sides of diaphragm; Stage IV refers to diffuse involvement of extra-lymphatic organ/sites aside from those specified "E," which references contiguous or proximal disease. More recently, the Lugano classification has been developed for assessment of staging and response, with stage I-II "limited disease," and stage III-IV "advanced disease" (44,50).

Nuclear medicine Gallium-67 imaging may be used for clinical staging, though inflammatory nodes and normal thymus may be confounding structures with uptake, and PET/CT is superior in terms of detecting musculoskeletal involvement (51). PET/CT is considered more accurate than CT for staging in both HL and NHL, as well as for assessing early response and end of treatment remission in lymphomas that were FDG-avid at baseline (44,50). PET/CT may upstage up to 33% of patients in comparison to CT alone (44). PET-CT is often used for treatment monitoring, though while the negative predictive value of maximum SUV no greater than mediastinal blood pool is high, the positive predictive value of diffuse or focal uptake in treated patients may be low, with Dunleavy *et al*. reporting a PPV of 17% (49).

Germ cell tumors (GCT)

In adults, the mediastinum is the most common location for extragonadal germ cell tumors (3). Germ cell tumors may be benign, such as teratomas or dermoid cysts, or malignant seminomatous or non-seminomatous germ cell tumors (NSGCT). Seminoma or mature teratoma are variably cited as the most common mediastinal germ cell tumor overall, with teratoma the most common mediastinal germ cell tumor in females (3). Mediastinal germ cell tumors are not associated with increased risk of gonadal germ cell tumors.

If germ cell origin is suspected, laboratory correlation with lactate dehydrogenase, alpha-fetoprotein, and beta-human chorionic gonadotropin (hCG) must be performed. Elevated HCG may cause gynecomastia or thyrotoxicosis (3).

Teratoma

Teratomas make up less than 10% of all mediastinal lesions, and occur with similar frequency in males and females (3).

Comprised of at least two germ cell layers (endoderm, mesoderm, ectoderm), they may show calcium, soft tissue, fat, and fluid (*Figure 10*). The majority, nearly 90%, have fluid attenuation or multilocular cystic portions. Calcification, which may be coarse, linear, rim or eggshell, has been reported in up to 53%, and bone or teeth in up to

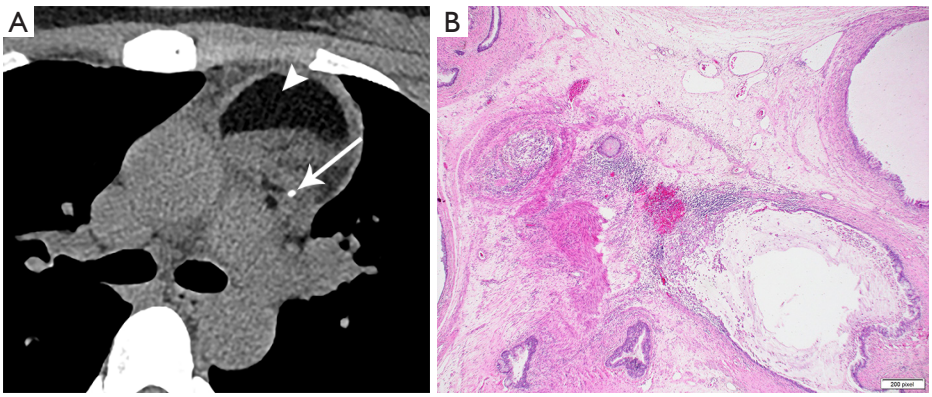

Figure 10 Teratoma. A 24-year-old woman with mass detected on chest radiograph. (A) Contrast enhanced axial CT image demonstrates a circumscribed left anterior mediastinal mass with components of varying density, including fat (arrowhead), soft tissue, and calcium (arrow), compatible with teratoma. (B) Histological sections show a tumor composed of disorganized mature epithelium, mesenchymal tissue, and neural tissue (H&E stain). It should be noted that not all elements need to be present to diagnose teratoma. The presence of a single type of squamous epithelium leads to the diagnosis of epidermoid cyst, a monophasic teratoma.

8% (3,8). A tooth would be considered a pathognomonic finding, and a fat-fluid level also a highly specific imaging finding. On MRI, fat saturation technique may reveal to better advantage any foci of macroscopic fat, and the presence of calcium should cause susceptibility artifact. Rupture into the pericardium or pleura can occur, indicated by adjacent pleuropericardial effusions.

Teratomas can be divided histologically into mature (containing mature adult type tissue) and immature (containing embryonal type tissue) subtypes. The histological diagnosis is characterized by the presence of multiple tissue types of epithelial, mesenchymal and neural origin. Skin and subcutaneous tissue are the most common findings, followed by respiratory and intestinal epithelium, fibroadipose tissue, smooth muscle, cartilage, nerve, and brain tissue. Immature teratomas show immature glands characterized by tall columnar cells, fetal lung mesenchymal cells, immature cartilage, and blast-like stroma. Neuroepithelial tissue is the most common.

Extensive examination of a teratomatous tumor is recommended to exclude the presence of non-teratomatous germ cell tumor elements. Whereas teratomas are treated by surgical excision alone, the presence of other germ cell tumor components requires systemic therapy.

Seminoma

Mediastinal seminomatous germ cell tumors are the most common single histology primary mediastinal germ cell tumors. Seminomatous GCTs occur almost exclusively in men, and in women are called dysgerminomas. The majority occur in young men 20–40 years of age (3). Beta-hCG is increased in approximately one third of patients, and LDH may also be elevated (3).

On imaging, these masses are usually large and homogeneous in appearance, with mild enhancement on contrast-enhanced CT (9) (*Figure 11*). However, they may less commonly also have multiloculated cystic components (3). On MRI, seminomas are T2 hypointense and septae enhance. Metastases are reported in 40% (3), and extrapulmonary metastases confer poor prognosis.

Non-seminomatous germ cell tumors (NSGCT)

Non-seminomatous germ cell tumors include embryonal carcinoma, yolk sac tumors, choriocarcinoma, and mixed germ cell tumors. While NSGCTs affect the same demographic as seminomas, they have different imaging features and behave more aggressively. Elevated tumor markers are common, such as elevated AFP in 80% (associated with yolk sac component), and beta-hCG in 30% (associated with choriocarcinoma component) (3); LDH may also be elevated.

On imaging, these appear as aggressive, heterogeneous soft tissue masses in the anterior mediastinum, often large and locally invasive. They are non-uniform in attenuation secondary to central areas of hemorrhage and necrosis, and peripheral areas of nodular enhancement (9). On MRI,

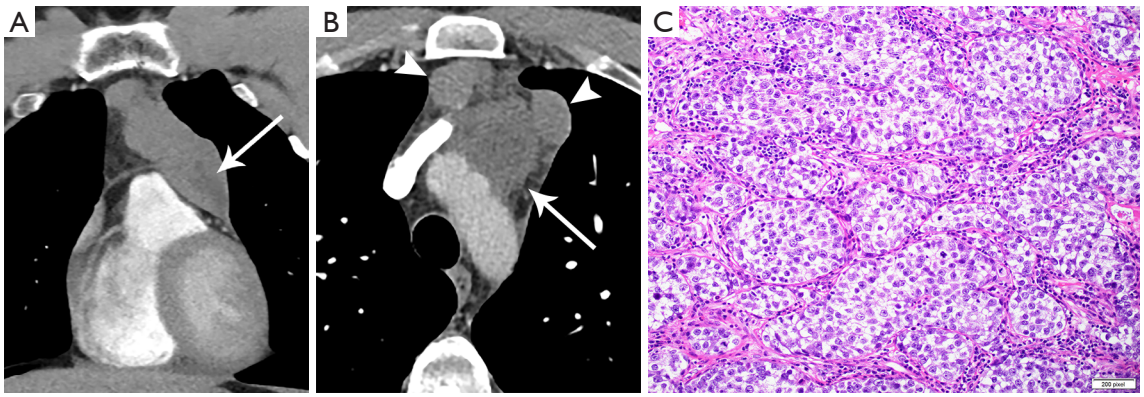

Figure 11 Seminoma. A 32-year-old man with pleuritic chest pain and elevated D-dimer. (A) Contrast enhanced coronal CT image demonstrates a large lobular anterior mediastinal mass with low level enhancement and hypo-attenuating cystic portions (arrow), though seminomas are more often homogeneous in comparison to non-seminomatous germ cell tumors. (B) Axial CT image demonstrates multiple mildly enlarged, enhancing anterior mediastinal lymph nodes (arrowheads), bordering the mildly enhancing and partially cystic mass (arrow). (C) Histological section shows a monomorphic tumor composed of large cells with prominent nucleoli and fragile cytoplasm (H&E stain). The cells have a "fried egg" appearance. Seminomas can show lymphocytic infiltrate and as well as small granulomatous inflammation adjacent to the tumor cells. Fibrosis can be prominent and lead to difficulty in diagnosing the tumor in small biopsies. Seminomas are positive by IHC for SALL 4, Oct4, D2-40, KIT and can be focally positive for keratin.

hemorrhagic foci appear T1 hyperintense. Signs of local invasion include pleural or pericardial fluid, thickening, or nodularity, lymphadenopathy, or direct pulmonary parenchymal extension.

Summary

Patient factors and clinical signs are often useful in the initial approach to anterior mediastinal lesions, given the varied demographic predilections and clinical presentations of these entities (52), including paraneoplastic syndromes. Laboratory workup when indicated, such as LDH, serum alpha fetoprotein, and beta-hCG, may also help narrow differential considerations.

Multimodality CT, MR, and nuclear medicine imaging often highlights distinguishing features among prevascular lesions, in addition to characterizing disease extent, which in some cases is sufficient for diagnosis and further management. Histopathology, with hallmark histologic and immunohistochemical findings, may definitively distinguish between lesions of thymic, lymphomatous, and germ cell origin, and guide systemic therapy when necessary.

Acknowledgments

Funding: None.

Footnote

Conflicts of Interest: All authors have completed the ICMJE uniform disclosure form (available at http://dx.doi.org/10.21037/med.2019.09.05). ALM serves as an unpaid editorial board member of *Mediastinum* from May 2017 to Apr 2019 and Jul 2019 - Jun 2021. The authors have no other conflicts of interest to declare.

Ethical Statement: The authors are accountable for all aspects of the work in ensuring that questions related to the accuracy or integrity of any part of the work are appropriately investigated and resolved.

References

1. Carter BW, Tomiyama N, Bhora FY, et al. A modern

definition of mediastinal compartments. J Thorac Oncol 2014;9:S97-101.
2. Araki T, Nishino M, Gao W, et al. Anterior Mediastinal Masses in the Framingham Heart Study: Prevalence and CT Image Characteristics. Eur J Radiol Open 2015;2:26-31.
3. Travis, WD, Brambilla, E, Burke, AP, et al. WHO Classification of Tumours of the Lung, Pleura, Thymus and Heart. Fourth. Lyon, France: International Agency for Research on Cancer, 2015.
4. Carter BW, Benveniste MF, Madan R, et al. IASLC/ITMIG Staging System and Lymph Node Map for Thymic Epithelial Neoplasms. Radiographics 2017;37:758-76.
5. Chaer R, Massad MG, Evans A, et al. Primary neuroendocrine tumors of the thymus. Ann Thorac Surg 2002;74:1733-40.
6. Gibril F, Chen YJ, Schrump DS, et al. Prospective Study of Thymic Carcinoids in Patients with Multiple Endocrine Neoplasia Type 1. J Clin Endocrinol Metab 2003;88:1066-81.
7. Araki T, Sholl LM, Hatabu H, et al. Radiological features and metastatic patterns of thymic neuroendocrine tumours. Clin Radiol 2018;73:479-84.
8. Moeller KH, Rosado-de-Christenson ML, Templeton PA. Mediastinal mature teratoma: imaging features. AJR Am J Roentgenol 1997;169:985-90.
9. Gu L, Zhang L, Hou N, et al. Clinical and radiographic characterization of primary seminomas and nonseminomatous germ cell tumors. Niger J Clin Pract 2019;22:342-9.
10. Nasseri F, Eftekhari F. Clinical and radiologic review of the normal and abnormal thymus: pearls and pitfalls. Radiographics 2010;30:413-28.
11. Carter BW, Marom EM, Detterbeck FC. Approaching the Patient with an Anterior Mediastinal Mass: A Guide for Clinicians. J Thorac Oncol 2014;9:S102-9.
12. Rosado-de-Christenson ML, Pugatch RD, Moran CA, et al. Thymolipoma: analysis of 27 cases. Radiology 1994;193:121-6.
13. Guimarães MD, Benveniste MFK, Bitencourt AG, et al. Thymoma originating in a giant thymolipoma: a rare intrathoracic lesion. Ann Thorac Surg 2013;96:1083-5.
14. Kaplan T, Han S, Han U, et al. Thymoma type B1 arising in a giant supradiaphragmatic thymolipoma. Asian Cardiovasc Thorac Ann 2014;22:1109-11.
15. Yvorel V, Forest F, Parietti E, et al. B3 thymoma arising within thymolipoma. Pathology 2015;47:702-5.
16. Carter BW, Benveniste MF, Madan R, et al. ITMIG Classification of Mediastinal Compartments and Multidisciplinary Approach to Mediastinal Masses. RadioGraphics 2017;37:413-36.
17. Shahrzad M, Le TSM, Silva M, et al. Anterior Mediastinal Masses. AJR Am J Roentgenol 2014;203:W128-38.
18. Detterbeck FC, Asamura H, Crowley J, et al. The IASLC/ITMIG Thymic Malignancies Staging Project: Development of a Stage Classification for Thymic Malignancies. J Thorac Oncol 2013;8:1467-73.
19. Engels EA. Epidemiology of Thymoma and Associated Malignancies. J Thorac Oncol 2010;5:S260-5.
20. Souadjian JV, Enriquez P, Silverstein MN, et al. The spectrum of diseases associated with thymoma. Coincidence or syndrome? Arch Intern Med 1974;134:374-9.
21. Levy Y, Afek A, Sherer Y, et al. Malignant thymoma associated with autoimmune diseases: a retrospective study and review of the literature. Semin Arthritis Rheum 1998;28:73-9.
22. Pirronti T, Rinaldi P, Batocchi AP, et al. Thymic lesions and myasthenia gravis. Diagnosis based on mediastinal imaging and pathological findings. Acta Radiol 2002;43:380-4.
23. Tomiyama N, Müller NL, Ellis SJ, et al. Invasive and noninvasive thymoma: distinctive CT features. J Comput Assist Tomogr 2001;25:388-93.
24. Marcus A, Narula N, Kamel MK, et al. Sensitivity and specificity of fine needle aspiration for the diagnosis of mediastinal lesions. Ann Diagn Pathol 2019;39:69-73.
25. Padda SK, Yao X, Antonicelli A, et al. Paraneoplastic Syndromes and Thymic Malignancies: An Examination of the International Thymic Malignancy Interest Group Retrospective Database. J Thorac Oncol 2018;13:436-46.
26. Asirvatham JR, Esposito MJ, Bhuiya TA. Role of PAX-8, CD5, and CD117 in Distinguishing Thymic Carcinoma From Poorly Differentiated Lung Carcinoma. Appl Immunohistochem Mol Morphol 2014;22:372-6.
27. Ackman JB, Kovacina B, Carter BW, et al. Sex difference in normal thymic appearance in adults 20-30 years of age. Radiology 2013;268:245-53.
28. Hara M, McAdams HP, Vredenburgh JJ, et al. Thymic hyperplasia after high-dose chemotherapy and autologous stem cell transplantation: incidence and significance in patients with breast cancer. AJR Am J Roentgenol 1999;173:1341-4.
29. Kissin CM, Husband JE, Nicholas D, et al. Benign thymic enlargement in adults after chemotherapy: CT demonstration. Radiology 1987;163:67-70.
30. Sun DP, Jin H, Ding CY, et al. Thymic hyperplasia after

chemotherapy in adults with mature B cell lymphoma and its influence on thymic output and CD4 + T cells repopulation. Oncoimmunology 2016;5:e1137417.
31. Sun DP, Wang L, Ding CY, et al. Investigating Factors Associated with Thymic Regeneration after Chemotherapy in Patients with Lymphoma. Front Immunol 2016;7:654.
32. Araki T, Sholl LM, Gerbaudo VH, et al. Imaging Characteristics of Pathologically Proven Thymic Hyperplasia: Identifying Features That Can Differentiate True From Lymphoid Hyperplasia. AJR Am J Roentgenol 2014;202:471-8.
33. Ackman JB, Verzosa S, Kovach AE, et al. High rate of unnecessary thymectomy and its cause. Can computed tomography distinguish thymoma, lymphoma, thymic hyperplasia, and thymic cysts? Eur J Radiol 2015;84:524-33.
34. Inaoka T, Takahashi K, Mineta M, et al. Thymic hyperplasia and thymus gland tumors: differentiation with chemical shift MR imaging. Radiology 2007;243:869-76.
35. Priola AM, Priola SM, Ciccone G, et al. Differentiation of Rebound and Lymphoid Thymic Hyperplasia from Anterior Mediastinal Tumors with Dual-Echo Chemical-Shift MR Imaging in Adulthood: Reliability of the Chemical-Shift Ratio and Signal Intensity Index. Radiology 2015;274:238-49.
36. Ackman JB, Mino-Kenudson M, Morse CR. Nonsuppressing normal thymus on chemical shift magnetic resonance imaging in a young woman. J Thorac Imaging 2012;27:W196-8.
37. Kumar A, Regmi SK, Dutta R, et al. Characterization of thymic masses using (18)F-FDG PET-CT. Ann Nucl Med 2009;23:569-77.
38. Endo M, Nakagawa K, Ohde Y, et al. Utility of 18FDG-PET for differentiating the grade of malignancy in thymic epithelial tumors. Lung Cancer 2008;61:350-5.
39. Jerushalmi J, Frenkel A, Bar-Shalom R, et al. Physiologic thymic uptake of 18F-FDG in children and young adults: a PET/CT evaluation of incidence, patterns, and relationship to treatment. J Nucl Med 2009;50:849-53.
40. Tomiyama N, Honda O, Tsubamoto M, et al. Anterior mediastinal tumors: Diagnostic accuracy of CT and MRI. Eur J Radiol 2009;69:280-8.
41. Gray GF, Gutowski WT. Thymoma. A clinicopathologic study of 54 cases. Am J Surg Pathol 1979;3:235-49.
42. Wernecke K, Vassallo P, Rutsch F, et al. Thymic involvement in Hodgkin disease: CT and sonographic findings. Radiology 1991;181:375-83.
43. Swerdlow SH, World Health Organization, International Agency for Research on Cancer. WHO classification of tumours of haematopoietic and lymphoid tissues [cited 2019 Jan 7]. Available from: http://publications.iarc.fr/Book-And-Report-Series/Who-Iarc-Classification-Of-Tumours/Who-Classification-Of-Tumours-Of-Haematopoietic-And-Lymphoid-Tissues-2017
44. Johnson SA, Kumar A, Matasar MJ, et al. Imaging for Staging and Response Assessment in Lymphoma. Radiology 2015;276:323-38.
45. Ackman JB. MR Imaging of Mediastinal Masses. Magn Reson Imaging Clin N Am 2015;23:141-64.
46. Hsu PK, Hsu HS, Li AF, et al. Non-Hodgkin's Lymphoma Presenting as a Large Chest Wall Mass. Ann Thorac Surg 2006;81:1214-8.
47. Savage KJ, Monti S, Kutok JL, et al. The molecular signature of mediastinal large B-cell lymphoma differs from that of other diffuse large B-cell lymphomas and shares features with classical Hodgkin lymphoma. Blood 2003;102:3871-9.
48. Rosenwald A, Wright G, Leroy K, et al. Molecular diagnosis of primary mediastinal B cell lymphoma identifies a clinically favorable subgroup of diffuse large B cell lymphoma related to Hodgkin lymphoma. J Exp Med 2003;198:851-62.
49. Dunleavy K, Pittaluga S, Maeda LS, et al. Dose-adjusted EPOCH-rituximab therapy in primary mediastinal B-cell lymphoma. N Engl J Med 2013;368:1408-16.
50. Barrington SF, Mikhaeel NG, Kostakoglu L, et al. Role of imaging in the staging and response assessment of lymphoma: consensus of the International Conference on Malignant Lymphomas Imaging Working Group. J Clin Oncol 2014;32:3048-58.
51. Sakurai M, Toyama T, Kikuchi T, et al. Comparison of fluorine-18 fluorodeoxyglucose positron emission tomography with gallium-67 scintigraphy in the initial clinical staging of diffuse large B-cell lymphoma. Int J Hematol 2018;107:194-200.
52. Carter BW, Okumura M, Detterbeck FC, et al. Approaching the Patient with an Anterior Mediastinal Mass: A Guide for Radiologists. J Thorac Oncol 2014;9:S110-8.

doi: 10.21037/med.2019.09.05
Cite this article as: Azour L, Moreira AL, Washer SL, Ko JP. Radiologic and pathologic correlation of anterior mediastinal lesions. Mediastinum 2020;4:5.